EL CARTEL O POSTER

La comunicación científica

Diego L. Linares

Por qué presentar un poster

- Es un método eficiente de presentación de trabajos académicos
- Puede tener más recordación que una presentación oral
- Permite presentar los primeros resultados de las investigaciones
- permite el acercamiento a los congresos por parte de los estudiantes.
- Es un excelente medio para presentar trabajos y generar oportunidades de trabajos en redes.

Característica Principal

- *Un poster debe ser tan claro que es entendible sin explicación verbal.*

Información dentro del Poster

- Sigue el clásico IMRAD (introducción, métodos, resultados y Discusión)

1. Título / Autor(es) / Centro(s)
2. Introducción, hipótesis y objetivo
3. Metodología (materiales y métodos)
4. Resultados
5. Conclusiones -Discusiones

Aspecto a tener en cuenta

1. El contenido: qué queremos decir a través del póster ("queremos presentar un estudio, una experiencia, un trabajo determinado")

2. La presentación: cómo vamos a presentarlo ("cómo vamos a estructurar la información").

El póster debe seguir una secuencia lógica que progrese de izquierda a derecha y de arriba abajo.

Formato de un poster académico

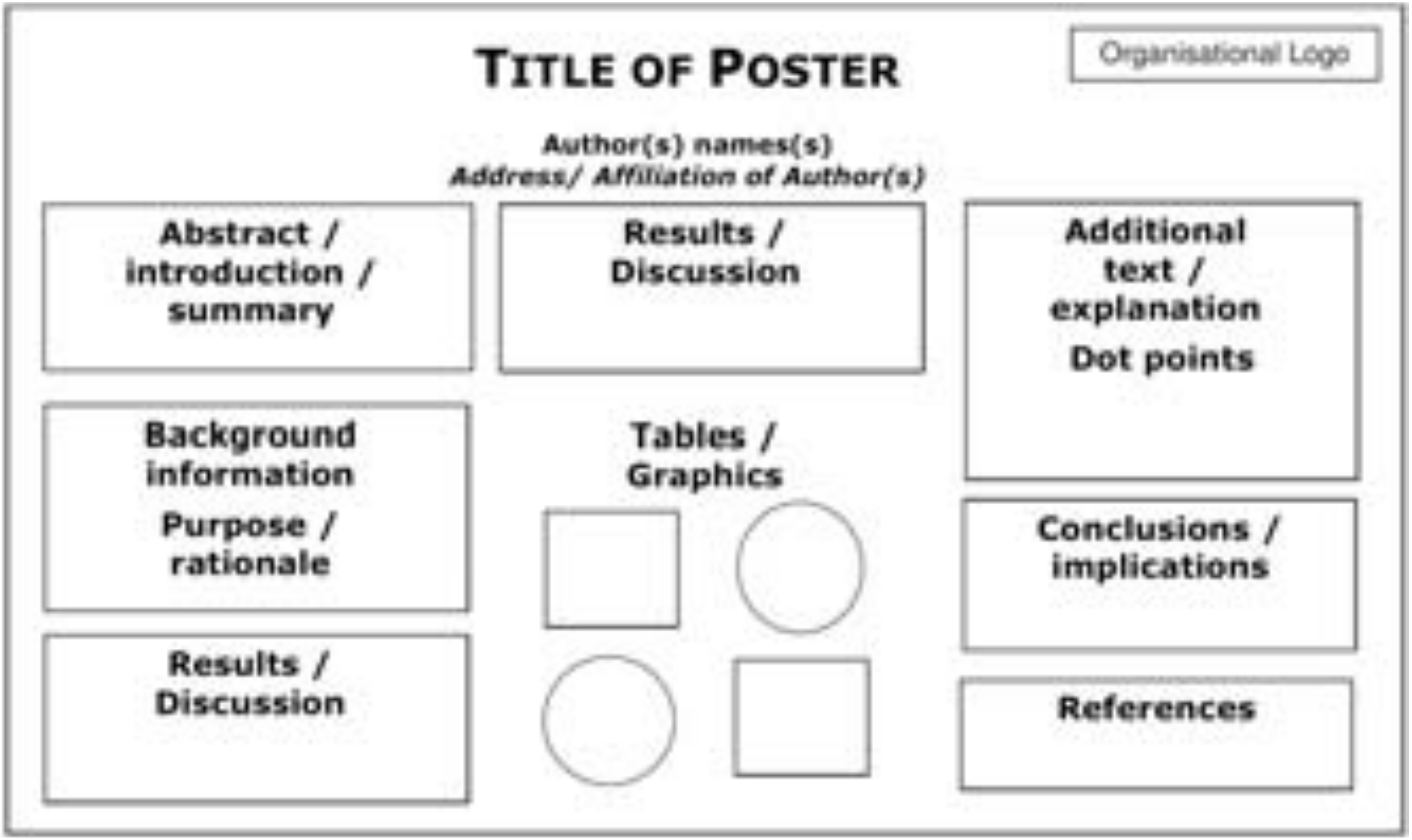

Pon aquí el título con letra grande y legible

Tu nombre aquí[1,2] y tus compañeros o profesor aquí [1], Departamento escolar[2], Nombre del colegio o instituto

ECOURBAN

RESUMEN

INTRODUCCIÓN Y ANTECEDENTES

METODOLOGÍA

METODOLOGÍA

RESULTADOS

RESULTADOS

CONCLUSIONES

PROPUESTAS DE FUTURO

AGRADECIMIENTOS:

Characterization of a Norovirus Strain from a 2004 Gastroenteritis Outbreak in a Maryland Hospital and its Comparison with Maryland Strains Circulating in 1987-88

Haoming Qiu[1], Kyeong-OK Chang[2], Gaël Belliot[2], Stanislav Sosnovtsev[2], Pat Rosenbaum[3], Patricia Lawson[3], Trish Perl[3], John Ticehurst[3], and Kim Y. Green[2]

[1] Department of Biology, Cornell University, Ithaca, NY
[2] Laboratory of Infectious Diseases, National Institute of Allergy and Infectious Diseases, NIH, DHHS, Bethesda, MD
[3] Johns Hopkins Medical Institutions, Baltimore, MD

Norovirus gastroenteritis has turned cruises from paradise into a struggle for bathroom space.

Introduction

Noroviruses are positive strand RNA viruses in the genus *Norovirus* of the family *Caliciviridae*. Other genera in the family include *Sapovirus*, *Vesivirus* and *Lagovirus*. Noroviruses are the predominant etiologic agents of nonbacterial epidemic gastroenteritis in the United States, causing an estimated 23 million cases annually [3].

Symptoms and Transmission

Symptoms of norovirus-related gastroenteritis include vomiting, diarrhea, abdominal cramping, and nausea. The symptoms are usually acute, lasting for a period of 24 to 60 hours with. Due to its environmental stability and high infectivity, Norovirus contamination of food and water can lead to large explosive outbreaks in settings such as schools, hospitals, social gatherings, recreational cruise ships, and nursing homes. Norovirus are also associated with large outbreaks on military bases and aircraft carriers. The virus is predominantly transmitted from person-to-person by the fecal-oral route [2].

History and Epidemiology

The prototype norovirus strain, Norwalk virus, was discovered as the agent of an outbreak of gastroenteritis in Norwalk, Ohio in 1968. The five genogroups (G) of *Norovirus* currently recognized are I through V. The GII/4 is currently the predominant genotype associated with human disease [4].

In 2002, a sharp increase in the number of norovirus outbreaks occurred in the United States and Europe. In both areas, the GII/4 norovirus strain responsible for the outbreaks appeared to be both more stable in the environment and more virulent [4,5]. In February of 2004, an outbreak of gastroenteritis occurred at the Johns Hopkins Hospital in Baltimore, Maryland causing severe gastroenteritis among patients and staff.

Research Objectives

The goal of this study was to characterize the strain of norovirus responsible for the outbreak at JHH and to compare its genome to a previous Maryland strain (MD-145, 1987) and to current predominant strains.

Materials and Methods

Stool Collection

Six stool specimens from patients who had contracted gastroenteritis were collected from the Coronary Care Unit at Johns Hopkins Hospital (JHH) during February, 2004. Viral RNA was extracted from stool specimens using the Qiagen RNeasy kit. Screening of samples positive for norovirus was accomplished with RT-PCR (with Invitrogen reagents) according to a method provided by the Centers for Disease Control and Prevention (Dr Stephan Monroe, personal communication). One sample was positive for norovirus. Preliminary sequence data indicated that the sample was a GII/4 virus. The virus in this sample was designated norovirus strain MD-2004 (Hu/NV/MD2004/US). Information concerning the outbreak was collected by the Hospital Epidemiology and Infection Control staff at JHH.

PCR Amplification of Viral Genome

A first strand cDNA synthesis from the viral RNA was performed using Super Script II Reverse Transcriptase and oligo dT for priming. A first round PCR was performed with *AmpliTaq* polymerase using 5'-end and 3'-end primers deduced from MD-145, a GII/4 strain of norovirus that was associated with gastroenteritis outbreaks in Maryland nursing homes from 1987-1988 [3]. A nested PCR approach was then used to amplify 1-2 kb overlapping fragments of the entire coding region of the genome of MD-2004. The amplified PCR DNA products were gel-purified and sequenced directly. Determination of the 5'- and 3'- ends are in progress.

Analysis

A BLAST nucleotide search was preformed with the sequence obtained from MD-2004. Nucleotide, amino acid and protein comparisons were performed using the ClustalW alignment program in the MacVector software package.

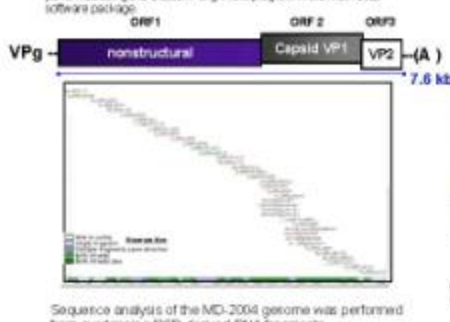

Sequence analysis of the MD-2004 genome was performed from overlapping PCR-derived DNA fragments.

Results

Epidemiological Data

- Outbreak took place February, 2004 in the Coronary Care Unit unit at JHH
- 41 individuals (75% staff) showed symptoms of gastroenteritis including nausea, vomiting and diarrhea.
- Patients were moved from the coronary care unit while it was disinfected.
- Concurrently, outbreaks of gastroenteritis with symptoms consistent with norovirus illness were reported throughout Northern Virginia in nursing homes and schools

Sequence Comparisons

Comparison of MD-2004 Genome with other GII/4 Strains

Name	Time	Place	GenBank #	% (Nt) Identity
1. Farmington Hills	2002	Michigan, USA	AY502023	99
2. Oxford	2002	England	AY587985	98
3. Langen	2002	Germany	AY485642	98
4. MD-145	1987	Maryland	AY032605	93
5. Camberwell	1994	Australia	AF145896	92

Comparison of Open Reading Frames (ORFs) of MD-2004 with other GII/4 Strains

Percent Nucleotide (Amino Acid) Identity

MD-2004	Farmington	Oxford	Langen	MD-145	Camberwell
ORF 1	99 (99)	98 (99)	98 (98)	93 (96)	92 (96)
ORF 2	99 (99)	98 (99)	98 (99)	93 (93)	93 (93)
ORF 3	98 (98)	98 (98)	98 (98)	91 (89)	90 (89)

Note: The 200 bp of the 3'-end of ORF 3 is not included in the analysis

Comparison of MD-2004 Nonstructural Proteins with GII/4 Strains

Percent Amino Acid Identity

	Farmington	Oxford	Langen	MD-145	Camberwell
N-Terminal	96	96	95	93	93
NTPase	100	100	99	97	97
p20	100	100	99	92	91
VPg	100	100	98	98	99
Proteinase	99	100	99	97	97
Polymerase	99	99	99	97	96

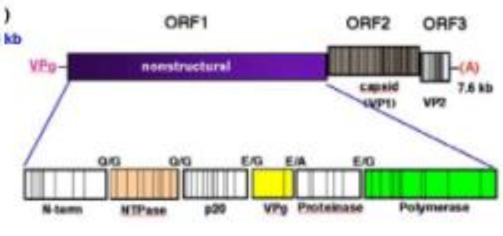

Analysis of amino acid substitutions between Maryland norovirus strains MD145 (1987) and MD-2004 (2004) show evidence for the evolution of a new GII/4 lineage.

Discussion

Norovirus Diversity

Preliminary analysis of the data shows that MD2004 is nearly identical to the new variant of GII/4 viruses discovered in 2002 such as Farmington Hills (US), Oxford (UK) and Langen (GE). MD2004 shows significant differences with MD-145, the predominant strain in Maryland in 1987-88. This is consistent with reports which indicate that norovirus strains appear to be epidemic on a global scale, with one strain predominating over a given period of time [2,4,5].

Genome Variation

The regions of the MD2004 genome which differ the most from MD-145 and other pre-2002 strains of norovirus are the ORF2 and ORF3. Variations in the ORF2 region might be expected since it encodes the capsid protein which is presumably under selective immune pressure [2]. In addition to several amino acid changes, Post-2002 strains, including MD-2004, have an amino acid insertion in the capsid domain that is believed to be responsible for neutralizing antibody and receptor attachment. The function of the ORF3 product, VP2, is unknown. However, some reports suggest that the VP2 protein may be responsible for virion stability [1]. Why this area should be highly variable among strains will require further investigation.

Inside the relatively conserved ORF1, the N-terminal protein and the p20 ("3A-like") protein show the highest variation. The functions of these protein are not known. Our recent studies indicate that this protein may interact with the Golgi apparatus. The p20 protein, like its counterpart in the picornavirus 3A, may also interact with cellular membranes during replication [2]. A key question is to determine whether variations in the nonstructural proteins are due to selective pressure that allows the virus to gain virulence.

Increased Virulence

It has been proposed that the post 2002 strains of norovirus have increased in virulence [4,5]. A recent report by the European Food-borne Viruses network shows large increases in norovirus outbreaks in England, Netherlands and Germany caused by the new 2002 GII/4 strain [4.] The CDC has also noted sharp increases in the number of norovirus outbreaks aboard cruise ships and in other settings in the United States associated with the closely related GII/4 strain Farmington Hills [5]. We show here that this GII/4 strain is still circulating in 2004 and associated with disease. How certain noroviruses adapt to become the predominant global strain remains an important question.

References & Acknowledgements

We would like to thank Dr. Albert Kapikian for his support and encouragement and Tanaji Mitra for his invaluable technical assistance.

1. Bertolotti-Ciarlet A, Crawford SE, Hutson AM, Estes MK. The 3' end of Norwalk virus mRNA contains determinants that regulate the expression and stability of the viral capsid protein VP1: a novel function for the VP2 protein. J Virol. 2003 Nov;77(21):11603-15
2. Green, KY, R.M. Chanock and A.Z. Kapikian. "Human Caliciviruses." Field's Virology 4th Edition. 2001
3. Green KY, Belliot G, Taylor JL, Valdesuso J, Lew JF, Kapikian AZ, Lin FY. A predominant role for Norwalk-like viruses as agents of epidemic gastroenteritis in Maryland nursing homes for the elderly. J Infect Dis. 2002 Jan 15;185(2):133-46
4. Lopman, B et al. Increase in viral gastroenteritis outbreaks in Europe and epidemic spread of new norovirus variant. Lancet. 2004 Feb 28;363(9410):682-8.
5. Widdowson, MA et al. Outbreaks of acute gastroenteritis on cruise ships and on land: identification of a predominant circulating strain of norovirus. J Infect Dis. 2004 Jul 1;190(1):27-36

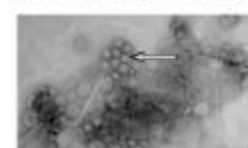

Norovirus (35,000x)

EM from Dave Bhella, University of Glasgow Medical Research Council

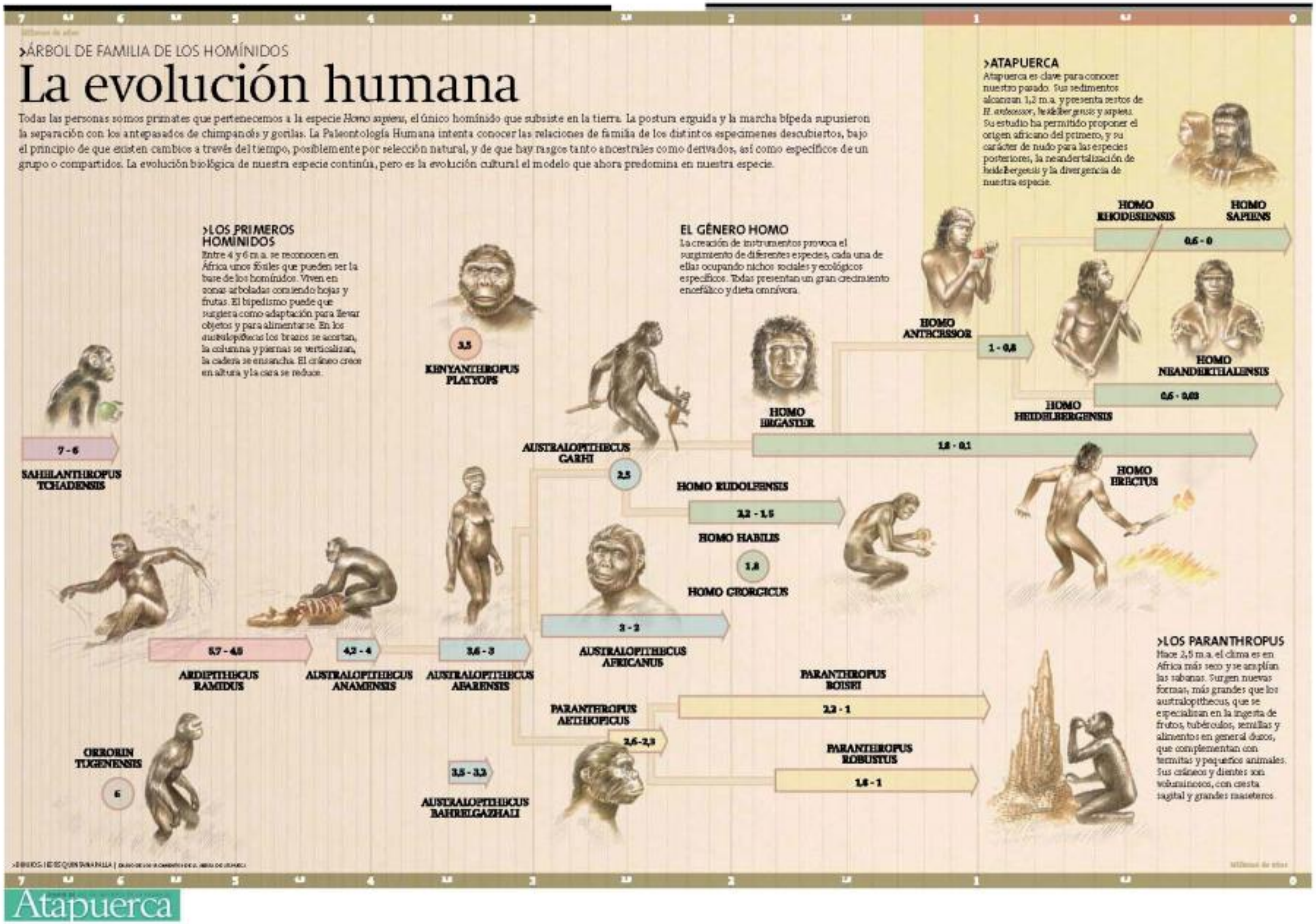

Fundación Atapuerca, Espacio Didáctico, Pósteres, http://www.atapuerca.org /

Developing and characterising a novel combined nanoelectrode system

L. P. Robinson, A. Mount

Electrochemistry at nanoelectrodes

Nanoelectrodes have several advantages for electrochemical sensing.

Linear diffusion profile

Transport to macroelectrodes proceeds through a relatively inefficient linear diffusion profile. They are also are highly affected by convection and iR drop.

In contrast, the diffusion pattern for nanoelectrodes quickly becomes hemispherical. This profile is much more efficient, and they are not so affected by convection or iR drop. They can reliably detect very low (attomole) concentrations of analyte.

Hemispherical diffusion profile

A Pt microsquare nanoband edge electrode (MNEE) array system in which the Pt nanoband acts as the working electrode has been developed. The project now aims to create a nanoelectrode device based on this system which has all three electrodes necessary for analysis on one chip.

Ag/AgCl as a combined electrode

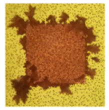

Dendritic growth

The combined reference/counter electrode is created by electroplating a thin film of Ag onto the Pt microsquare.

Potentiostatic plating causes Ag to grow preferentially at the corners, creating dendrites. A galvanostatic plating protocol is being developed to provide the required smooth, shiny Ag deposit.

To convert the newly plated Ag surface to AgCl, it must be functionalised. Chemical functionalisation by immersion in $FeCl_3$ has been shown to produce uniform deposits of AgCl.

Combined nanoelectrode system

This design consists of a microsquare at the bottom of each cavity in the array, with the nanoband around the cavity edge.

The Ag/AgCl microsquare is a combined reference and counter electrode. As its area is so much larger than the Pt nanoband, the current passing through the square is not large enough to affect its use as the reference electrode.

This could create an on-chip device for sensitive analytical detection.

Characterisation

Cyclic voltammetry and electrochemical impedance spectroscopy will be used to verify that the system is behaving as predicted. The nanoband should have a similar reponse to the current nanoelectrode array.

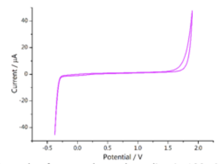

Example of a nanoelectrode cycling in 100mM KCl solution. This cycle is used to determine the cleanliness of the electrode surface.

Fabrication

This design has been fabricated at the Scottish Microelectronics Centre using photolithography. In this technique layers of metal and insulator are deposited and patterned to produce the desired arrangement.

1. Si wafer with oxide surface

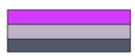

2. Metal is then deposited and coated in a nitride passivation layer

3. Photoresist layer is deposited and exposed to UV light through a patterned mask

4. Nitride is removed and process repeated to pattern metal layer

Each layer is deposited and patterned sequentially. This approach reliably produces uniform electrodes cheaply and easily.

An application

By coating the surface of the working electrode in a probe nucleic acid, the corresponding DNA sequence can be detected using electrochemical impedance spectroscopy (EIS). Before the target molecule is hybridised, the resistance measured for the redox couple is small. When the correct target is hybridised the resistance, and therefore the EIS reponse, is much larger.

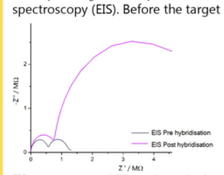

EIS measurement of 50 nm electrode shows the increase in resistance upon addition of the target nucleic acid.

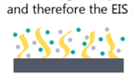

Pre hybridisation - the redox species has access to the electrode.

Post hybridisation - the access of the redox species is restricted, and so the resistance rises at the electrode.

Objectives

Having made the initial measurements, the next steps will include;

- complete fabrication of the combined system, including optimisation of nanoband and cavity dimensions
- further investigation of the sensitivity of nanoelectrodes for use in DNA sensing and the relationship between the response and concentration of the target
- optimisation of a galvanostatic silver plating protocol

Many thanks to Dr Damion Corrigan, Ilka Schmueser, Professor Andy Mount, the Mount group and the SMC for their continuing support and expertise.

SMC

EPSRC
Pioneering research and skills

Quantum non-Gaussian character of a heralded single-photon state

Miroslav Ježek, Ivo Straka, Michal Mičuda, Miloslav Dušek, Ladislav Mišta, Jr., Jaromír Fiurášek, Radim Filip

Department of Optics, Faculty of Science, Palacký University, 17. listopadu 12, 77900 Olomouc, Czech Republic

Abstract

We report on the experimental verification of quantum non-Gaussian character of a heralded single-photon state with a positive Wigner function. We unambiguously demonstrate that the generated state cannot be expressed as a mixture of Gaussian states. Sufficient information to witness the quantum non-Gaussian character is obtained from a standard photon anticorrelation measurement.

Experimental verification of quantum non-Gaussianity

Heralded single-photon source is based on parametric down-conversion process in 2 mm thick beta-barium borate (BBO) pumped by 50 mW cw multimode laser diode at 407 nm.

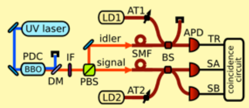

Photon pairs are separated from the pump by a dichroic mirror (DM) and spectrally limited by an interference filter (IF). The orthogonally polarized photons of a PDC pair are separated by a polarizing beam splitter (PBS) and coupled to single-mode optical fibers (SMF). Both outputs can be mixed with an attenuated (AT) laser diode (LD) signal at fiber beam splitters (BS) to emulate dark counts of detectors and a noise component of the state. The output modes are detected by single-photon detectors (APD) with efficiency of 50%. Electronic dark counts in coincidence basis were found to be completely negligible. The coincidence circuit (5 ns coincidence window) operates on output channels TR, SA, SB.

Each data set $[R_0, R_{1A,B}, R_2]$ yields the corresponding probabilities $[p_0, p_1]$, from which we have calculated $\Delta W = ap_0 + p_1 - W_G(a)$ and maximized the difference over all a. The resulting maximal criterion violation $\Delta W > 0$ in all cases and the bound $W_G(a)$ is always surpassed by many standard deviations [4],

P [mW]	IF [nm]	p_0	p_1	ΔW [$\times 10^{-6}$]
50	2	0.9124	0.0875	412 ± 1
50	10	0.8589	0.1410	1666 ± 3
20	10	0.8425	0.1574	2370 ± 2
50	–	0.7095	0.2901	14252 ± 17
5	–	0.7296	0.2704	11825 ± 15

Quantum non-Gaussianity under noisy conditions

We have investigated the influence of background noise on the source properties. For this purpose we inject light from laser diodes LD1 and LD2 into trigger and signal detection blocks, respectively. Noise from LD2 emulates noise of the source while noise coming from LD1 effectively increases dark count rate of the trigger. With increasing noise in the both blocks we observe transition to the regime where $\Delta W < 0$,

n_{rel}	p_0	p_1	a_{opt}	ΔW [$\times 10^{-6}$]
0.0	0.8195	0.1804	0.94018	3479 ± 7
0.1	0.9073	0.0926	0.98389	406 ± 3
0.2	0.9408	0.0591	0.99332	42 ± 2
1.0	0.9777	0.0222	0.99903	-84 ± 1

All the results exhibit strong photon anti-correlation effect [5] witnessed by $\frac{R_0 R_2}{R_{1A} R_{1B}} < 0.37$, including the case $n_{\mathrm{rel}} = 1$ for which $\Delta W < 0$:

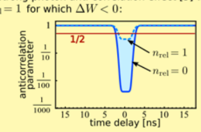

Non-Gaussian character of the state is strongly affected by multiphoton content. We have studied its dependence on the noise amount added to the trigger channel only (green circles) and to both the channels simultaneously (red squares). All other parameters were fixed, P=50 mW and IF=10 nm.

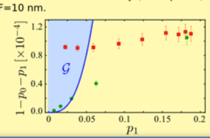

Motivation and theoretical background

Which mixed non-classical quantum states with positive non-Gaussian Wigner function do not admit explanation based solely on stochastic non-Gaussianity?

Negativity of Wigner function is equivalent to quantum non-Gaussian character of a pure state [1] but this relation does not simply extend to mixed states [2]. Its experimental verification also requires complete information on the state. Under lossy conditions, the negativity cannot be observed directly even for highly non-Gaussian states such as an arbitrary superposition of single photon and vacuum.

Recently, a criterion of the quantum non-Gaussianity has been theoretically proposed [3]. It is based on knowledge of probabilities of vacuum and single-photon states only, yet it can detect a wide class of states with positive Wigner function which are not mixtures of Gaussian states.

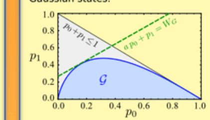

The boundary of Gaussian set $\mathcal{G}$ is given by the upper limit on the probability p_1 of single photon for a given probability p_0 of vacuum,

$$p_0 = \frac{e^{-d^2[1-\tanh(r)]}}{\cosh(r)} \qquad p_1 = \frac{d^2\, e^{-d^2[1-\tanh(r)]}}{\cosh^3(r)}$$

(r: squeezing parameter, $d^2 = \frac{e^{4r}-1}{4}$: displacement)

We define a non-Gaussianity witness $W(a) = ap_0 + p_1$. All points $[p_0, p_1]$ lying in the half-plane $ap_0 + p_1 > W_G(a)$, $W_G(a) = \max_{\rho \in \mathcal{G}} W(a)$, are certified by the witness to correspond to a state $\rho \notin \mathcal{G}$.

Using binary detectors (APD) and common Hanbury-Brown--Twiss correlation measurement, we are able to estimate probability of vacuum and lower bound of single-photon probability,

$$p_0 = 1 - \frac{R_{1A} + R_{1B} + R_2}{R_0}$$

$$p_1 = \frac{R_{1A} + R_{1B}}{R_0} - \frac{T^2 + (1-T)^2}{2T(1-T)} \frac{R_2}{R_0} \leq p_{1,\mathrm{true}}$$

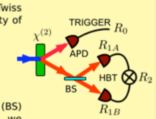

(R_0: # of states, $R_{1A,B}$: single rates, R_2: coincidences)
We assume an arbitrary splitting ratio of the beam splitter (BS) and unity detection efficiency. For realistic detector, we underestimate the single-photon contribution further.

Conclusion

We have examined a source producing approximate single-photon states with positive Wigner function but exhibiting strong photon anti-correlation and we have unambiguously proved that the generated states cannot be expressed as mixtures of Gaussian states. In comparison to the witness based on negativity of the Wigner function, the present criterion can identify quantum non-Gaussianity of a much wider class of single photon sources. Consequently, the presented criterion is particularly useful for evaluation of single-photon sources where negativity of Wigner function cannot be observed.

Outlook: Schrödinger cat and quantum dot

In collaboration with A. Tipsmark, R. Dong and U.L. Andersen, DTU Physics, Kgs. Lyngby: Approximate coherent cat state is prepared by subtracting a single-photon from squeezed vacuum and measured by means of balanced homodyne detection. Vacuum and single-photon contribution are estimated employing direct reconstruction from raw data. We have demonstrated statistically significant quantum non-Gaussianity even for states with positive Wigner function.

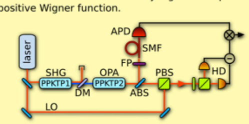

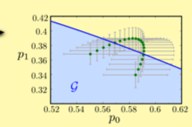

In collaboration with A. Predojevic, T. Huber, H. Jayakumar and G. Weihs, Uni of Innsbruck: The emission from InAs/GaAs quantum dot is spectrally filtered. Generated biexciton and exciton photons are coupled to single-mode (SMF) and multi-mode (MMF) fibers, respectively. Exciton emission is split in a multimode fibre beamsplitter to estimate vacuum and single-photon contributions. Non-Gaussian character is witnessed by $\Delta W > 0$.

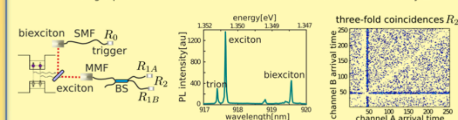

References

[1] R. L. Hudson, Rep. Math. Phys. 6, 249 (1974).
[2] A. Mandilara, E. Karpov, and N. J. Cerf, Phys. Rev. A 79, 062302 (2009).
[3] R. Filip and L. Mišta, Jr., Phys. Rev. Lett. 106, 200401 (2011).
[4] M. Ježek, I. Straka, M. Mičuda, M. Dušek, J. Fiurášek, and R. Filip, Phys. Rev. Lett. 107, 213602 (2011).
[5] P. Grangier, G. Roger and A. Aspect, Europhys. Lett. 1, 173 (1986).

Acknowledgments: The work was supported by Projects No. MSM6198959213, No. LC06007 and ME10156 of the Czech Ministry of Education, by Palacký University (PrF-2012-019) and by Czech Science Foundation (202/09/0747).

Preparar un poster

- Considerar la audiencia
- Dedicarle tiempo, un buen poster toma tiempo elaborarlo
- Conozca claramente los requerimientos del congreso donde lo va a presentar.
- Conozca los criterios de evaluación del poster y del resumen (si son evaluados)
- Revise otros poster para inspirarse: diseño, claridad, formato y calidad en general.
- Decida el método, puede ser utilizando un formato prehecho (latex, ppt, etc..) o contratando un diseñador.

Diseñando el poster

- Considere el mensaje que desea desarrollar
- Realice varios borradores, esto le dará una idea realista de cómo se verá su poster al final.
- Revise continuamente la claridad y la precisión del lenguaje usado, la claridad de las figuras, la ortografía, etc..
- Ubíquese a tres metros de distancia y revise:
  - El mensaje es claro y accesible
  - Hay un buen balance entre texto y gráficos
- Evite Abreviaciones, acrónimos, y jerga, las palabras técnicas se pueden usar, pero asegúrese que su audiencia le entenderá, sino incluya las definiciones, de manera apropiada, en el lugar necesitado.

80-96 puntos para títulos

30-36 para encabezados

18-24 para textos

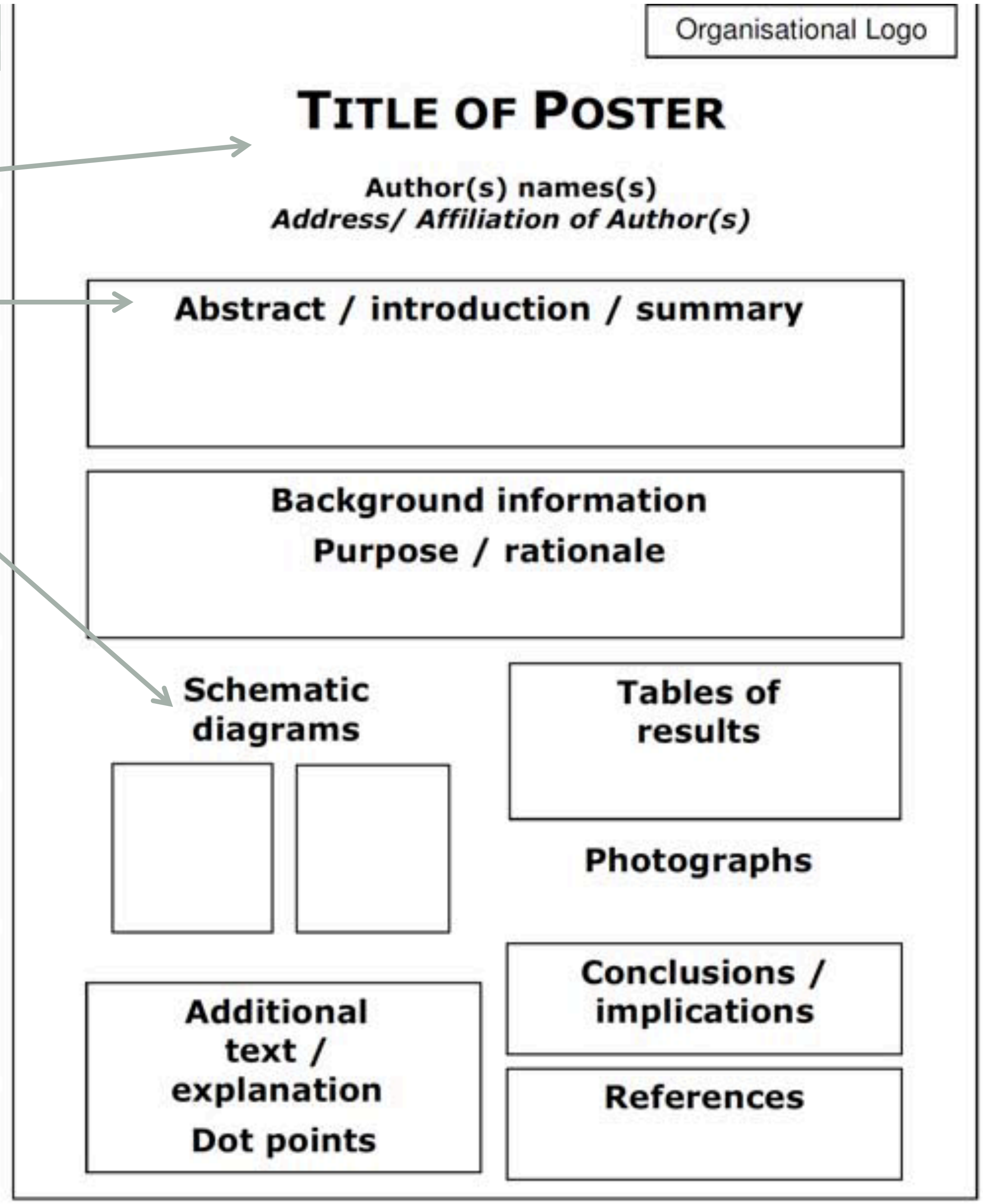

Recomendaciones:

- La selección de colores debe ser simple y agradable a la vista: máximo tres colores
- Minimizar el uso de **Negritas**, subrayados, *itálicas,* resaltados
- Incluya áreas vacías

Recursos:

(recuperados el 5 de abril de 2017)

Formatos en ppt
https://www.posterpresentations.com/html/free_poster_templates.html

Formato en latex:
https://www.latextemplates.com/cat/conference-posters

Creating Effective Poster presentation:
https://projects.ncsu.edu/project/posters/

Bibliografía:

Academic poster:
http://services.unimelb.edu.au/__data/assets/pdf_file/0007/470059/Academic_posters_Update_051112.pdf